KINETICS AND MECHANISMS OF ELECTROCHEMICAL REACTIONS ON PLATINUM WITH SOLUTIONS OF IODINE–SODIUM IODIDE IN ACETONITRILE*

V. A. Macagno, M. C. Giordano

Departamento de Fisicoquímica, Instituto de Ciencias Químicas, Universidad
Nacional de Córdoba, Córdoba, Argentina

and

A. J. Arvía

Instituto Superior de Investigaciones, Facultad de Química y Farmacia,
Universidad Nacional de La Plata, La Plata, Argentina

Abstract—The kinetics of the iodine–tri-iodide–iodide electrode in acetonitrile has been investigated in the temperature range from 0 to 30°C. Current/voltage curves were determined using a platinum rotating disk electrode working at 200 to 3000 rpm. The anodic and cathodic current/voltage curves are characterized by two well defined waves. The total reactions related to the first and second anodic waves are respectively

$$3I^- = I_3^- + 2 e$$

and

$$2I_3^- = 3I_2 + 2 e,$$
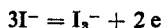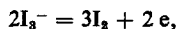
while the reverse reactions represent the second and first cathodic waves respectively. The diffusion coefficients of the diffusing species have been evaluated.

Current/voltage curves in the region preceding the limiting cd exhibit a measurable irreversibility. The kinetic parameters related to the activated process were determined, and the kinetics of the reactions interpreted in terms of reaction mechanisms that involve an ion plus atom reaction as rate determining step for the anodic process and the reverse reaction for the cathodic process.

Résumé—La cinétique de l'électrode d'iode, tri-iodure, iodure dans l'acétonitrile a été étudiée a des températures comprises entre 0 et 30°C. Les courbes courant/voltage furent déterminées en employant une électrode de disque tournant de platine fonctionnant de 200 jusqu'a 3000 tours p.m. Les courbes courant/voltage anodiques etc athodiques sont caratérisées pard eux vagues bien définies. Les réactions totales par rapport aux première et deuxième vagues anodiques sont respectivement:

$$3I^- = I_3^- + 2 e$$

et

$$2I_3^- = 3I_2 + 2 e,$$
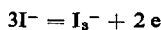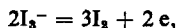
tandis que les réactions inverses représentent les deuxième et première vagues cathodiques respectivement. Les coefficients de diffusion des différentes espèces ont été évalués.

Les courbes courant/voltage dans la région qui précède la densité limite du courant montrent une irréversibilité considérable. On a déterminé les paramètres cinétiques relatifs au processus activé et la cinétique des réactions a été interpretée sur la base de mécanismes de réaction comprenant une réaction d'ion plus atome comme étape régulatrice dans le processus anodique et la réaction inverse pour les processus cathodique.

Zusammenfassung—Die Kinetik der Iod/Triiodid/Iodid-Elektrode wurde bei Temperaturen von 0 bis 30°C untersucht. Mit einer rotierenden Scheibenelektrode aus Platin wurden Strom/Spannungs-kurven im Bereich von 200 bis 3000 UpM aufgenommen. Die anodische und die kathodische Strom/ Spannungskurve werden durch zwei definierte Wellen charakterisiert. Die Gesamtreaktionen für die beiden anodischen Wellen sind:

$$3I^- \rightarrow I_3^- + 2 e$$

und

$$2I_3^- \rightarrow 3I_2 + 2 e$$
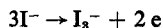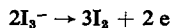
während die beiden kathodischen Wellen von den Rückreaktionen herrühren. Die Diffusions-koeffizienten der verschiedenen Teilchen wurden bestimmt.

335

Die Strom/Spannungskurven weisen unterhalb des Grenzstromes eine messbare Irreversibilität auf. Die kinetischen Parameter des aktivierten Prozesses wurden bestimmt. Für die Reaktionen wurden Mechanismen angenommen, die als geschwindigkeitsbestimmenden Schritt im anodischen Vorgang eine Ion-plus-Atom-reaktion, und die umgekehrte Reaktion im kathodischen Vorgang enhalten.

INTRODUCTION

The electrochemical behaviour of the iodine–iodide electrode was investigated in different organic solvents, covering a wide range of dielectric constants.[1] The polarographic study of those systems showed the existence of two polarographic waves related to both the anodic and cathodic processes.

Some recent investigations[2,3] on the kinetics of the electrode reactions involving the iodine–iodide couple in dimethylsulphoxide (DMSO) on platinum electrodes showed that appreciable activation polarization contributions are involved, and the evaluation of the kinetic parameters made it possible to interpret those electrode reactions in terms of a reaction scheme comprising an electron-transfer reaction as the rate determining step.

As far as those results are concerned it was thought that they were not limited to DMSO solutions and that a similar behaviour could be expected in other organic solvents. Therefore it was interesting to attempt to elucidate the kinetics of the iodine–tri-iodide–iodide electrode in acetonitrile (ACN), which is also an aprotic solvent having at 20°C a dielectric constant of 36 and a viscosity of 3.45×10^{-3} poise at 25°C.

Previous voltammetric studies[4] on platinum electrodes of solutions containing iodine, sodium iodide and trimethyl ammonium tri-iodide in ACN demonstrated that the current/voltage curves involved at least two well-defined waves, both for the anodic and cathodic reactions. The total reactions related to each wave were definitely established, indicating that the current/voltage curves were more complex than the expectations for a simple reversible electrode process.

More recently,[5] the difference of half-wave potentials deduced from the two anodic waves determined during the voltammetric oxidation of iodide to iodine in nitromethane, in acetone and in ACN as solvents, on a platinum-wire rotating electrode, was related to the magnitude of the stability constant of tri-iodide ion in those solvents.

On the basis of these previous studies and taking into account that the stability constant related to tri-iodide ion formation in ACN is known,[6,7] the present paper refers to experiments involving both the kinetic study of the anodic and cathodic processes occurring on a rotating platinum-disk electrode, in order to deduce the likely mechanisms of the reactions.

EXPERIMENTAL TECHNIQUE

The arrangement of the experimental set-up was essentially the same as previously described.[2] To obtain reproducible results the platinum working electrode was carefully polished with a suspension of alumina in alcohol before each run. The rotation speed of the disk was changed from 200 to 3000 rpm. Its constancy was maintained within 0·5 per cent by means of an electronic control of the driving motor.[8]

As reference electrode, either a platinum electrode dipped into the redox system or a silver/silver-iodide electrode was used. The latter was prepared by electrolysing a solution of sodium iodide in ACN, employing a silver anode and a platinum cathode.

Electrolyte solutions were prepared from analytical reagents. The ACN (Carlo Erba) was conveniently purified by successive distillations at a reduced pressure, the vapour passing through dry potassium hydroxide. Solvent purification and solution preparation were made in an all glass apparatus under a dry nitrogen atmosphere.

Solutions prepared either with iodine, iodide or with both chemicals were employed. For the latter, the ratio of iodine to iodide was varied from 0·05 to 3 thereabouts. The concentrations of the solutions used were evaluated by conventional analysis. Viscosities of some solutions are shown in Table 1.

TABLE 1. VISCOSITY OF SOLUTIONS
25°C C_{NaClO_4}, 0·4 M

C_{I_2} M	C_{NaI} M	$\nu \times 10^2$ cm²/s
—	0·00367	0·4908
0·0230	0·0273	0·4911
—	0·0287	0·4999
0·1280	0·0323	0·4927
0·0151	0·0081	0·5034

Sodium perchlorate was employed as supporting electrolyte; its concentration was about 0·4 M. Experiments were performed in the temperature range from 0 to 30 ± 0·1°C.

RESULTS

Current/voltage curves were obtained either potentiostatically or galvanostatically at different rotation speeds and temperatures, covering a voltage range of about 3 V, according to the electrochemical stability of the solvent. Between successive runs at a constant rotation speed, the working electrode becomes more polarizable, causing a shift of current/voltage curves. This effect, caused by some sort of film formation on the electrode surface, was minimized by polishing the working electrode before each run. It was reflected in the non-coincidence of current/voltage curves traced by changing the current upwards or downwards. The current/voltage curves are shown in Figs. 1–4, corresponding to the anodic as well as the cathodic reactions under a wide range of experimental conditions. The overvoltage, η, is defined as the absolute difference between the actual electrode potential E, related to apparent cd I, and the equilibrium electrode potential, E_r.

As shown in Fig. 5, the hysteresis effect is particularly remarkable in the second cathodic wave. Current/voltage curves traced back exhibit, at constant current, a larger overvoltage than that obtained when the curves are traced in the forward direction. The hysteresis loop is more marked at longer sweeping times, as shown in Fig. 6.

At the highest negative potentials once the limiting current of the second cathodic wave is reached, an appreciable decrease of current occurs, the electrode approaching a passive state. It is interesting to see that the electrode passivation disappears if oxygen is bubbled though the solution during the cathodic experiments.

The anodic and cathodic current/voltage curves involve two well defined waves, in the potential range investigated, as early observed in the voltammetric study of iodine–iodide solutions in ACN.[4] When solutions containing an excess of iodide are
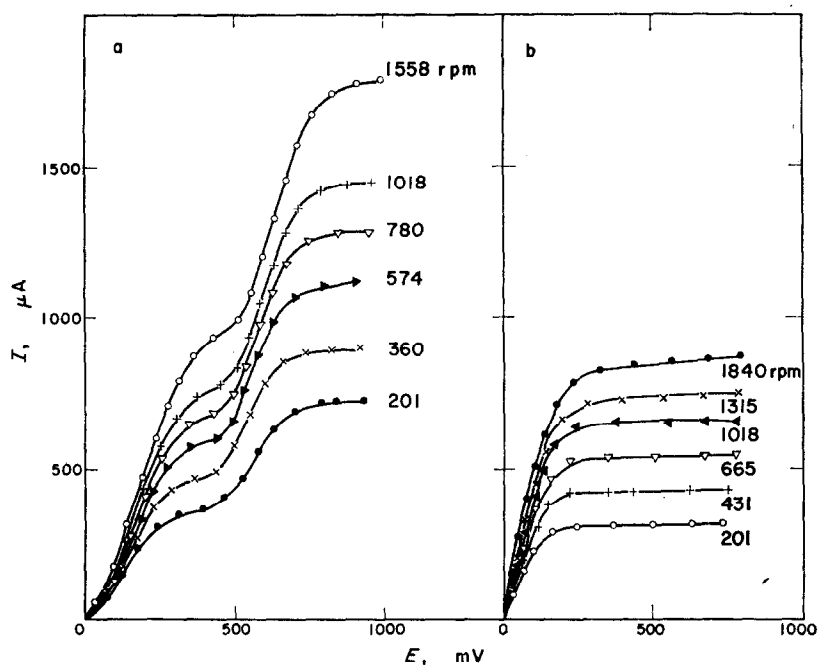
FIG. 1. Anodic current/voltage curves.
a, $C_{I_2} = 0.0023$ M; $C_{NaI} = 0.0244$ M; $C_{NaClO_4} = 0.4$ M; 25.2°C.
b, $C_{I_2}^- = 0.0208$ M; $C_{NaI} = 0.0097$ M; $C_{NaClO_4} = 0.4$ M; 25.0°C.

FIG. 2. Anodic current/voltage curves.
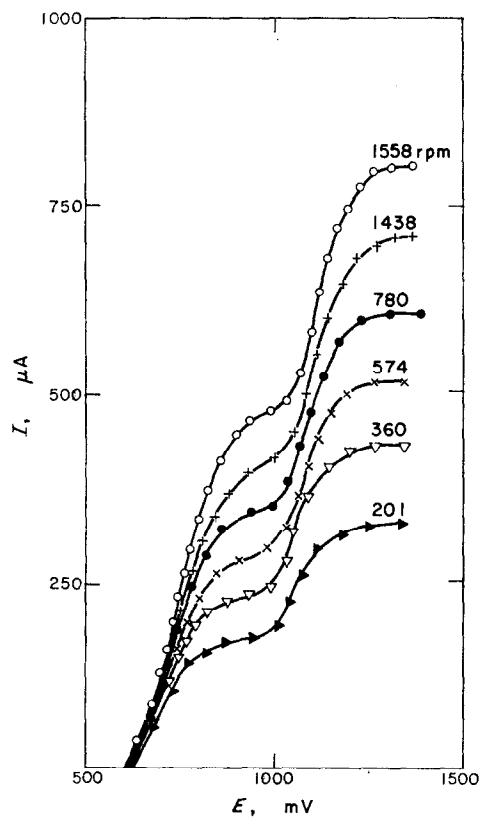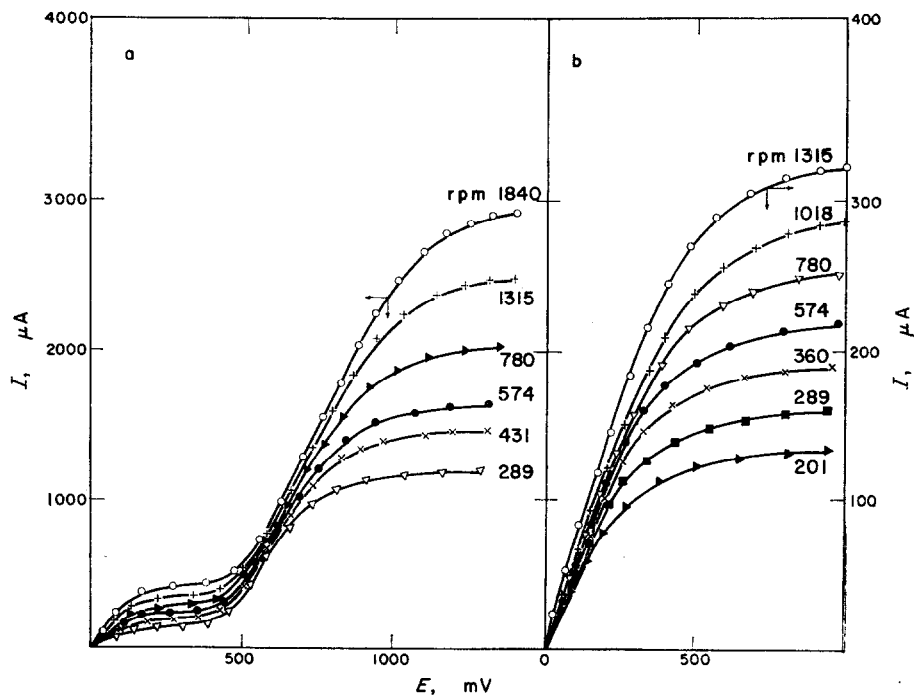$C_{NaI} = 0.0095$ M. Ag/AgI reference electrode; $C_{NaClO_4} = 0.4$ M. 30.2°C.

FIG. 3. Cathodic current/voltage curves.
a, $C_{I_2} = 0.0185$ M; $C_{NaI} = 0.0110$ M; 25·1°C.
b, $C_{I_2} = 0.0023$ M; $C_{NaI} = 0.0244$ M; 25·4°C.
$C_{NaClO_4} = 0.4$ M.
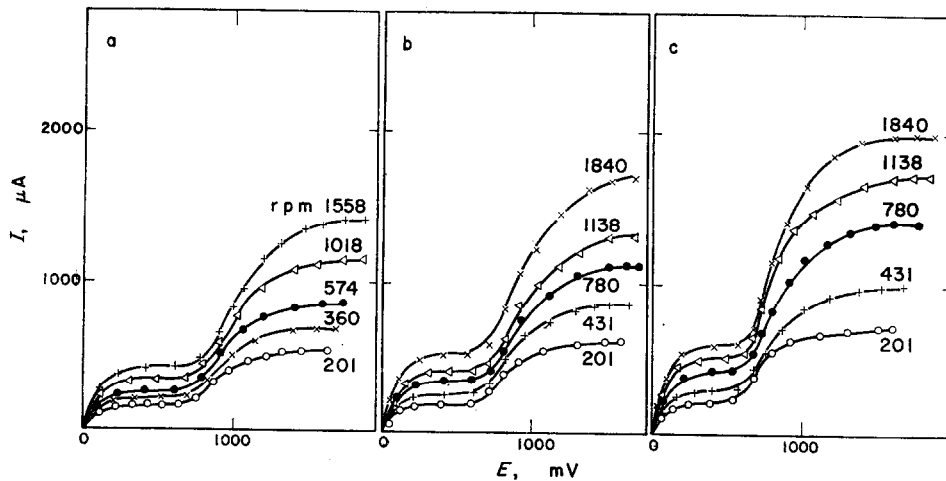
FIG. 4. Cathodic runs at different temperatures.
$C_{I_2} = 0.0093$ M; $C_{NaClO_4} = 0.4$ M.
a, 0°C; b, 11·7°C; c, 28·5°C.
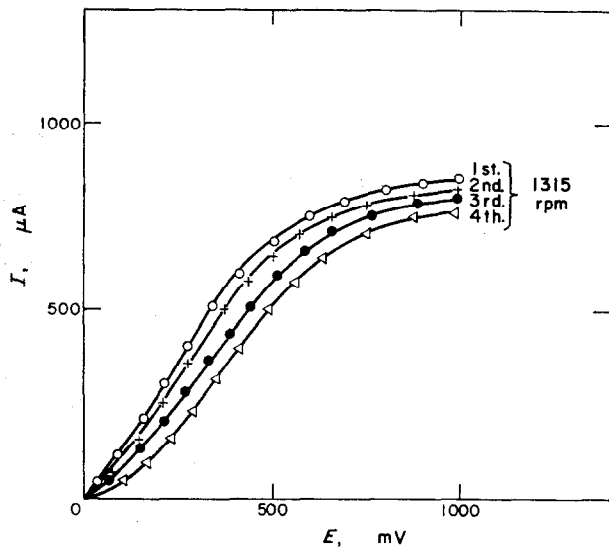
FIG. 5. Successive cathodic runs without polishing the working electrode.
$C_{I_2} = 0.0071$ M; $C_{NaI} = 0.0304$ M; $C_{NaClO_4} = 0.4$ M. 25.0°C.

FIG. 6. Cathodic current/voltage curves obtained by changing current upwards and downwards, with different sweep times as indicated.
$C_{I_2} = 0.0071$ M; $C_{NaI} = 0.0304$ M; $C_{NaClO_4} = 0.4$ M. 25.0°C.

used, two anodic waves and only one cathodic wave are observed, whereas if an excess of iodine is present, two cathodic waves and only one anodic wave are observed.

The four limiting currents, at a constant composition, increase linearly with the square root of the rotation speed, ω(rad/s), as shown in Figs. 7–10.

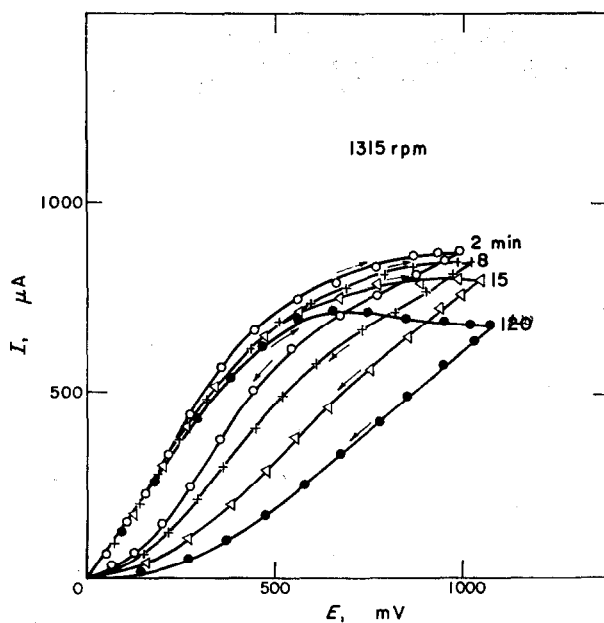When solutions containing plain iodine are used, the first and second cathodic limiting currents, at a constant rotation speed, increase linearly with iodine concentration, whereas, when solutions containing plain iodide are used, the anodic limiting currents increase linearly with iodide concentration.
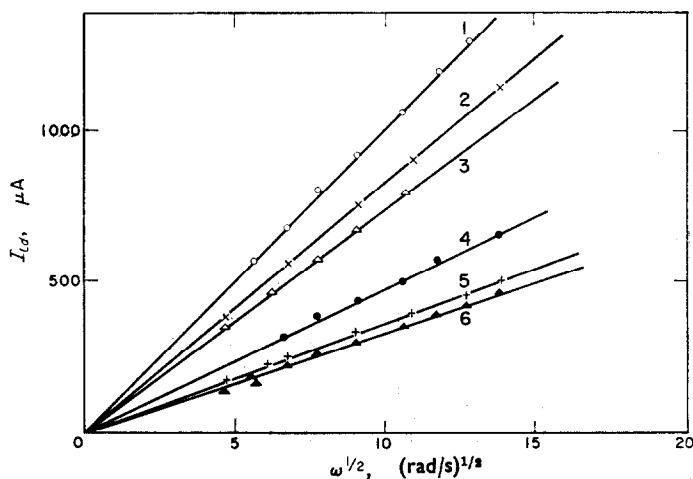
FIG. 7. Dependence of the first anodic limiting current on $\omega^{1/2}$.
$C_{NaClO_4} = 0.4$ M. $25.0°C$

	C_{I_2}	C_{NaI}
1	0.0073 M	0.0305 M
2	0.0024 M	0.0275 M
3	—	0.0184 M
4	0.0023 M	0.0244 M
5	—	0.0080 M
6	0.0187 M	0.0252 M

In the case of solutions containing iodine and iodide at any ratio, the only limiting current, either anodic or cathodic, which is observed, depending on the species in excess, also increases linearly with the concentration of the latter. The concentration dependence of the limiting currents is shown in Fig. 11.

The limiting currents increase with temperature and these dependences fit Arrhenius plots. The experimental activation energies, ΔE_a, related to the convective diffusion processes are assembled in Table 2.

INTERPRETATION AND DISCUSSION

The total electrode reactions

Iodide ion, iodine and tri-iodide ion dissolved in ACN are the three reacting species that participate in the electrochemical reactions, being related by the equilibrium

$$I^- + I_2 = I_3^-. \tag{1}$$
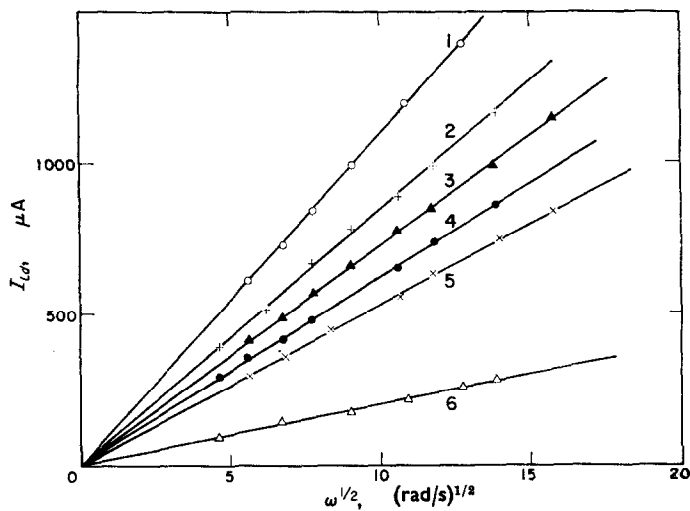
FIG. 8. Dependence of the second anodic limiting current on $\omega^{1/2}$
$C_{NaClO_4} = 0.4$ M. 25.0°C

	C_{I_2}	C_{NaI}
1	0.0730 M	0.0305 M
2	0.0148 M	0.0127 M
3	0.0185 M	0.0110 M
4	0.0208 M	0.0097 M
5	0.0151 M	0.0081 M
6	—	0.0081 M
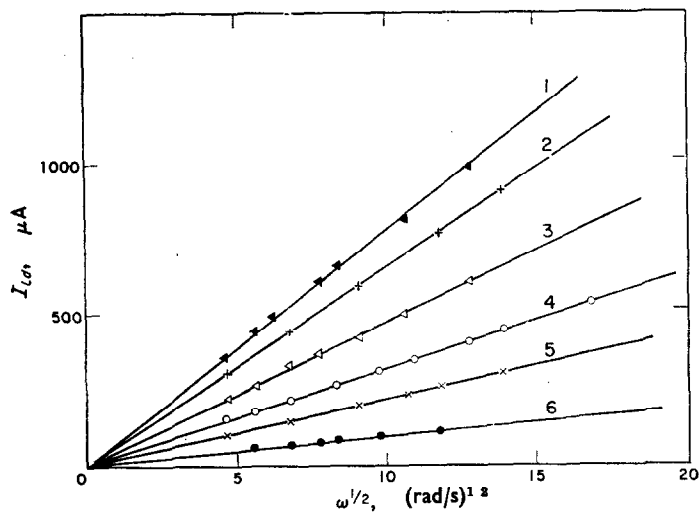
FIG. 9. Dependence of the first cathodic limiting current on $\omega^{1/2}$.
$C_{NaClO_4} = 0.4$ M. 25°C

	C_{I_2}	C_{NaI}
1	0.0160 M	—
2	0.0133 M	—
3	0.0208 M	0.0097 M
4	0.0151 M	0.0081 M
5	0.0177 M	0.0124 M
6	0.0148 M	0.0127 M
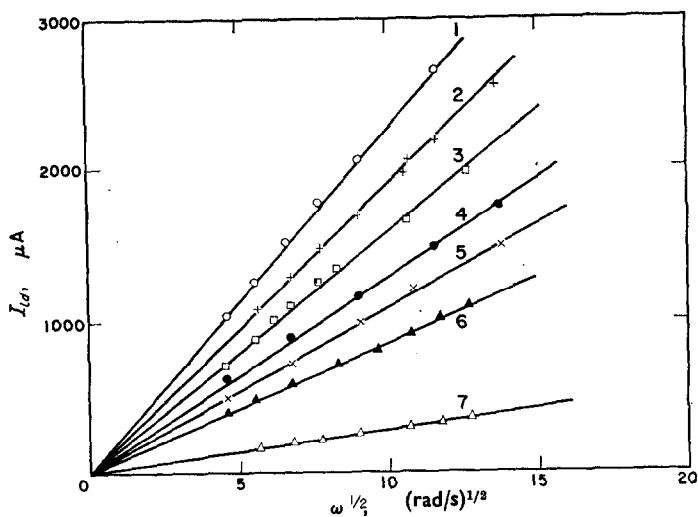
FIG. 10. Dependence of the second cathodic limiting current on $\omega^{1/2}$.

$C_{NaClO_4} = 0.4$ M.   25°C

	C_{I_2}	C_{NaI}
1	0.0200 M	0.0122 M
2	0.0151 M	0.0250 M
3	0.0160 M	—
4	0.0133 M	—
5	0.0093 M	—
6	0.0073 M	0.0315 M
7	0.0024 M	0.0275 M
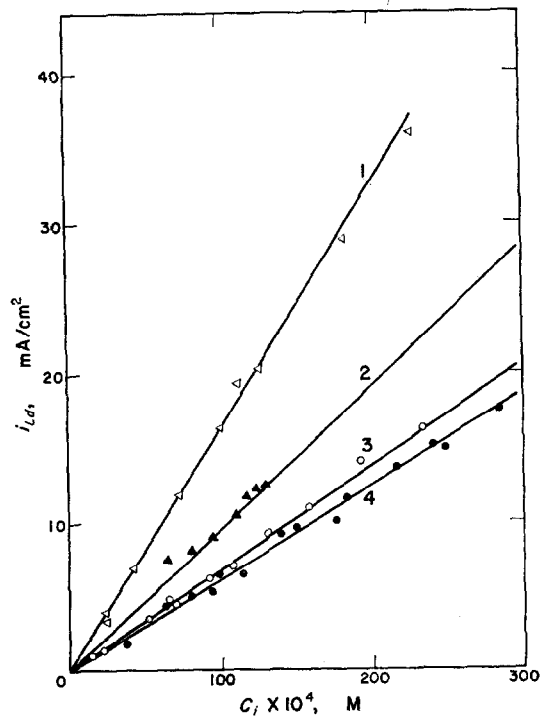
FIG. 11. Dependence of the limiting cd on concentration of reacting species.
1, 2nd cathodic l.cd vs $C_{I_3^-}$.   3, 1st cathodic l.cd vs free iodine concentration.
2, 2nd anodic l.cd vs $C_{I_3^-}$ 4, 1st anodic l.cd vs free iodide-ion concentration.

Table 2. Experimental activation
energies related to the
convective–diffusion processes

$(\Delta E_a)_{1a}$	1700 ± 500 cal/mol
$(\Delta E_a)_{2a}$	1900 ± 500 cal/mol
$(\Delta E_a)_{1c}$	1950 ± 500 cal/mol
$(\Delta E_a)_{2c}$	2000 ± 500 cal/mol

Its equilibrium constant, is about 10^7 at $25°C$,[6] so that it is much higher than that corresponding to the equilibrium in aqueous solutions. Hence, equilibrium (1) in ACN is markedly shifted towards tri-iodide ion formation, as compared to aqueous solutions. This fact is responsible for the existence of the two waves both in the anodic and cathodic/current voltage curves. For the solutions containing iodide only, the following total reactions are related to the first and second anodic waves, respectively,[4]

$$3I^- = I_3^- + 2e \tag{2}$$

and

$$2I_3^- = 3I_2 + 2e. \tag{3}$$

Similarly, the following total reactions are involved in the first and second cathodic waves, respectively, particularly for those solutions containing only iodine,

$$3I_2 + 2e = 2I_3^- \tag{4}$$

and

$$I_3^- + 2e = 3I^-. \tag{5}$$

When solutions containing different ratios of iodide to iodine are employed, in general three of the four reactions (2) to (5) occur. If the iodide/iodine concentration ratio is greater than 1, no appreciable iodine concentration exists and the current/voltage curve is characterized by the appearance of two anodic waves related respectively to reactions (2) and (3) and only one cathodic wave corresponding to reaction (5). If that concentration ratio is less than 1, the iodide-ion concentration is negligible, yielding consequently two cathodic waves related to reactions (4) and (5) and only one anodic step related to reaction (3).

According to reactions (2) to (5), if the limiting currents are due to convective-diffusion controlled processes, as a first approximation the following conclusions may be drawn. The first anodic limiting current should increase linearly with the iodide-ion concentration. The first cathodic limiting current should increase linearly with the iodine concentration, and, finally, the second anodic and cathodic limiting currents should depend linearly on tri-iodide ion concentration. The latter, taking into account the magnitude of the equilibrium constant of (1), must be taken as equal to the iodine concentration in the solutions containing an excess of iodide ion, while it must be taken as equal to the iodide-ion concentration in the solutions containing an excess of iodine. These interpretations are in good agreement with the experimental results shown in Fig. 11.

Evaluation of diffusion coefficients

The linear dependence of the limiting currents on the square root of rotation speed, at constant composition and temperature, indicates a convective–diffusion kinetic control, at least within their corresponding overvoltage regions. Therefore,

from that relationship and the application of Levich's equation for the rotating disk electrode for the kind of process,[9] the diffusion coefficients of the iodide ion, iodine and tri-iodide ion in ACN can be evaluated. The diffusion limiting current, $I_{l,d}$, is related to the diffusion coefficients $D_i(cm^2/s)$ of the reacting species, i, by

$$I_{l,d} = 0.62nFD_i^{2/3}\omega^{1/2}C_{0,i}\nu^{-1/6}A, \tag{6}$$

ν being the kinematic viscosity of the solution (cm^2/s), n the number of electrons per mol deduced from the corresponding total reaction, $C_{0,i}$ the bulk concentration of i $(mole/cm^3)$, and A the apparent electrode area (cm^2). Values of D_i for the three species are shown in Table 3, where the Einstein–Stokes ratios, $D\eta/T$, and solvodynamic radii, r_i, are also assembled.

TABLE 3

Species	Wave	Total reaction	n	$D_i \times 10^5$ cm^2/s	$D_i\eta/T \times 10^{10}$ $g\,cm^2/s^2\,°K$	r_i Å
I^-	Anodic (1)	$3I^- = I_3^- + 2\,e$	2/3	1·68	2·31	3·17
I_2	Cathodic (1)	$3I_2 + 2\,e = 2I_3^-$	2/3	1·91	2·61	2·80
I_3^-	Cathodic (2)	$I_3^- + 2\,e = 3I^-$	2	1·37	1·88	3·89
I_3^-	Anodic (2)	$2I_3^- = 3I_2 + 2\,e$	1	1·55	2·13	3·44

The diffusion coefficients of the reacting species in ACN solutions are larger than those earlier found for those species in DMSO solutions, as a consequence mainly of the lower viscosity of the former solvent.

The iodine Einstein–Stokes radius is very close to the radius of the iodine molecule $(r_{c,I_2} = 2.67\,Å)$, suggesting a likely participation of a bare iodine molecule in the cathodic process occurring at lower overvoltage. The larger Einstein–Stokes radii of the iodide and triiodide ions should be related to its solvation state in the ACN solutions.

Departure from a purely convective–diffusion control

If currents read at a fixed potential, in the overvoltage region preceding the limiting current region, are plotted against the square root of the rotation speed, a clear departure from a straight line is observed, as would correspond to a purely convective–diffusion-controlled process. These deviations, which are shown in Figs. 12 and 13, are definite indications of the existence of an activation polarization contribution in the electrode processes.[9,10]

To evaluate the contribution of each polarization, the results are treated with the equations derived for intermediate kinetic processes occurring on a rotating disk electrode. For this case, the relationship between the cd and the rotation speed, with first-order kinetics, is given by the equation:

$$\frac{1}{I} = \frac{1}{I_L} + \frac{1}{B\omega^{1/2}}, \tag{7}$$

where I_L is the maximum cd approached when the rotation speed becomes infinite; B is a constant that depends on the concentration of the diffusion species, being equal to $I_{l,d}/\omega^{1/2}$. When $\omega \rightarrow \infty$, the rate process comes only under a kinetic control, depending on the electrochemical reactions occurring within the electrical double
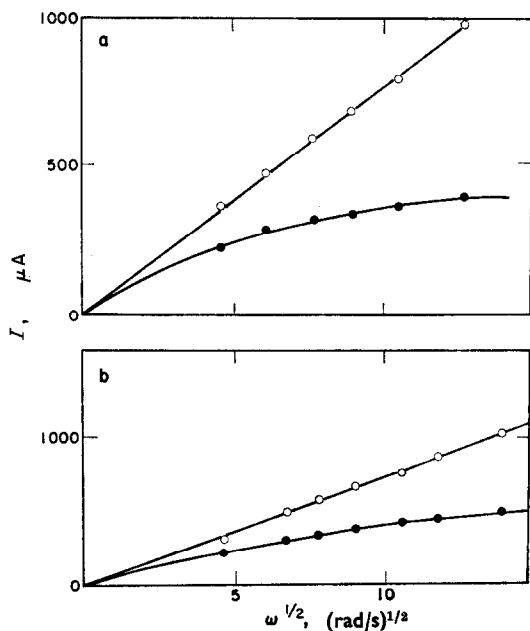
Fig. 12. Plots of I vs $\omega^{1/2}$.

a, First anodic wave. $C_{I_2} = 0{\cdot}0023$ M; $C_{NaI} = 0{\cdot}0244$ M; $C_{NaClO_4} = 0{\cdot}4$ M. 25·2°C; $\eta_k = 160$ mV.   b,   Second   anodic   wave. $C_{I_2} = 0{\cdot}0185$ M; $C_{NaI} = 0{\cdot}0110$ M; $C_{NaClO_4} = 0{\cdot}4$ M; 25·0°C; $\eta_k = 100$ mV.

Fig. 13. Plots of I vs $\omega^{1/2}$.

a, First cathodic wave. $C_{I_2} = 0{\cdot}0133$ M; $C_{NaClO_4} = 0{\cdot}4$ M; 25·0°C; $\eta_k = 100$ mV.
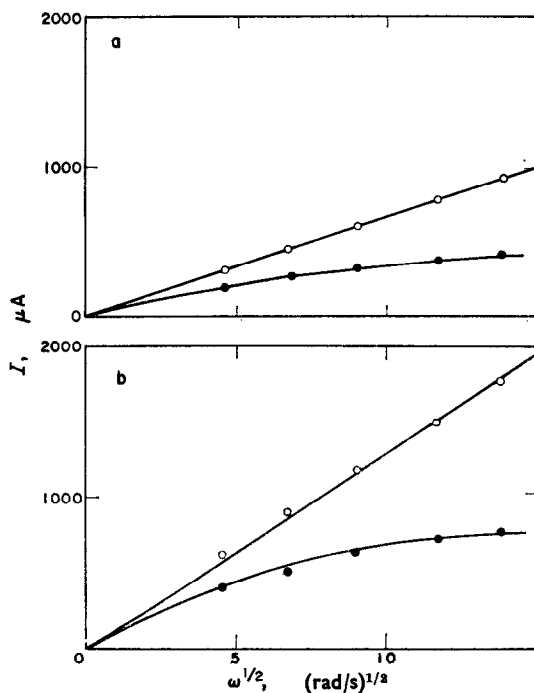b, Second cathodic wave. $C_{I_2} = 0{\cdot}0133$ M; $C_{NaClO_4} = 0{\cdot}4$ M; 23·1°C; $\eta_k = 100$ mV.
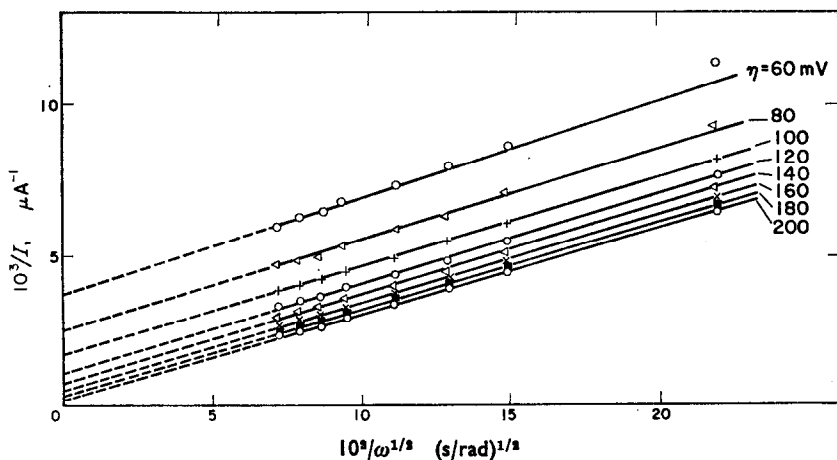
FIG. 14. Plot of $1/I$ vs $1/\omega^{1/2}$. Oxidation of iodide ion.
$C_{I_2} = 0.0187$ M; $C_{NaI} = 0.0252$ M; $C_{NaClO_4} = 0.4$ M. 25°C.
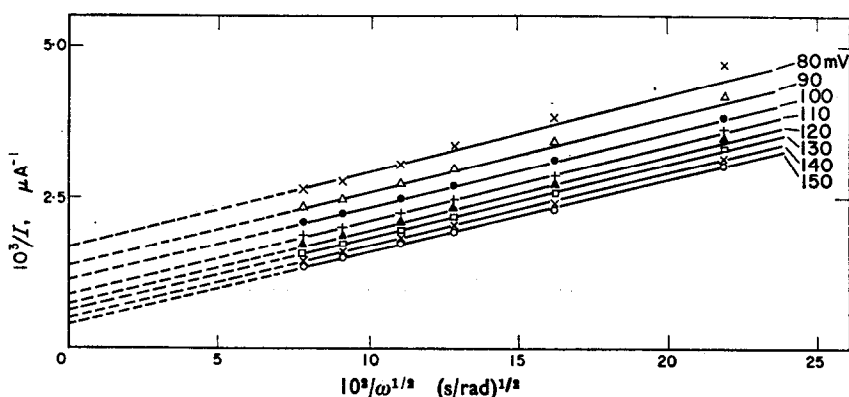
FIG. 15. Plot of $1/I$ vs. $1/\omega^{1/2}$. Oxidation of tri-iodide ion.
$C_{I_2} = 0.0200$ M; $C_{NaI} = 0.0122$ M; $C_{NaClO_4} = 0.4$ M. 24.9°C.

layer. When this situation is reached the concentration of the reacting species on the electrode surface becomes equal to its concentration in the bulk of the solution.

If the reaction orders are either 0·5 or 2, the corresponding equations relating current and rotation speed are respectively

$$I^2 = I_L^2 - \left(\frac{I_L^2}{B}\right)\left(\frac{I}{\omega^{1/2}}\right) \tag{8}$$

and

$$I^{1/2} = I_L^{1/2} - \left(\frac{I_L^{1/2}}{B}\right)\left(\frac{I}{\omega^{1/2}}\right). \tag{9}$$

Equations (7), (8) and (9) were compared with the experimental results. With data taken at high overvoltages, (7) yields a good straight line at a fixed overvoltage when $1/I$ is plotted against $1/\omega^{1/2}$, having a slope $1/B$. These sets of straight lines are shown in Figs. 14–17.

5
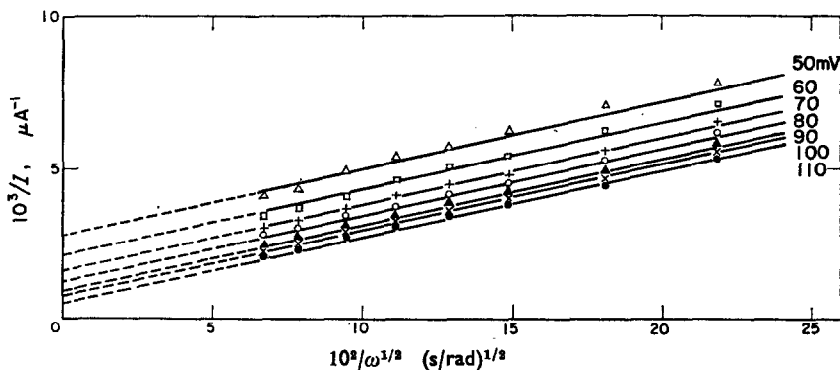
FIG. 16. Plot of $1/I$ vs $1/\omega^{1/2}$. Reduction of iodine.
$C_{I_2} = 0.0208$ M; $C_{NaI} = 0.0097$ M; $C_{NaClO_4} = 0.4$ M. 25.0°C.
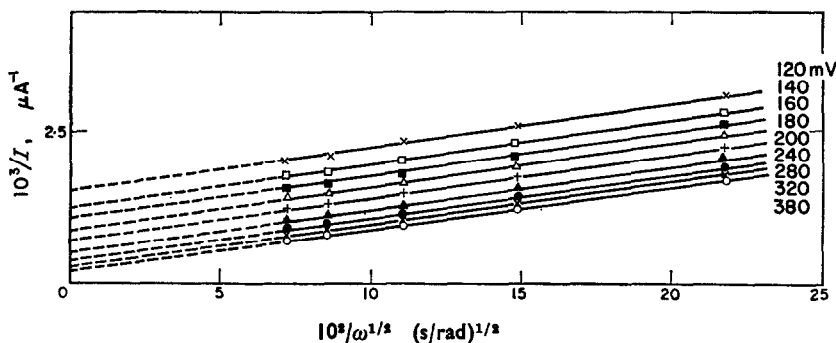
FIG. 17. Plot of $1/I$ vs $1/\omega^{1/2}$. Reduction of tri-iodide ion.
$C_{I_2} = 0.0133$ M. $C_{NaClO_4} = 0.4$ M. 25°C.

In the application of this calculation procedure a further correction, involving the pseudo-ohmic drop, was made. As a matter of fact, the I_L values are actually related to an overvoltage which comprises an ohmic contribution. The latter was evaluated from

$$\frac{\partial \eta}{\partial I_L} = \frac{b_T}{I_L} + R, \tag{10}$$

as described in a previous publication.[2] The pseudo-ohmic resistance in the present case was about 40 Ω. After the proper correction, the actual activation polarization, η_k, was known and plotted according to Tafel's equation

$$(\eta_k)_x = -\frac{RT}{(\alpha)_x F} \ln (I_0)_x + \frac{RT}{(\alpha)_x F} \ln I_x, \tag{11}$$

as shown in Figs. 18–21. $(I_0)_x$ and $(\alpha)_x$ are respectively the exchange cd and transfer coefficient of process x. The kinetic parameters derived from the experimental results, including the reaction order, p, obtained from Figs. 18 and 21, and the Tafel slopes, b_T, are assembled in Tables 4 and 5. The activation energies calculated from the
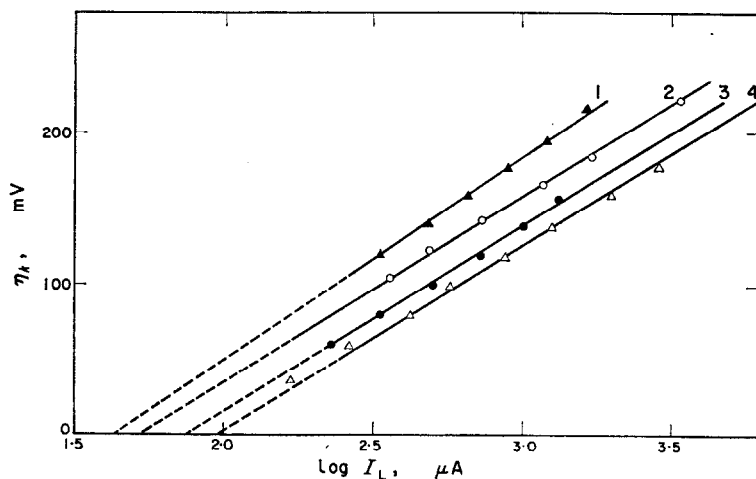
FIG. 18. Tafel plots. Oxidation of iodide ion.
$C_{NaClO_4} = 0.4$ M. 25°C.

	C_{I_2}	C_{NaI}
1	0·0023 M	0·0244 M
2	—	0·0080 M
3	0·0113 M	0·0251 M
4	0·0187 M	0·0252 M
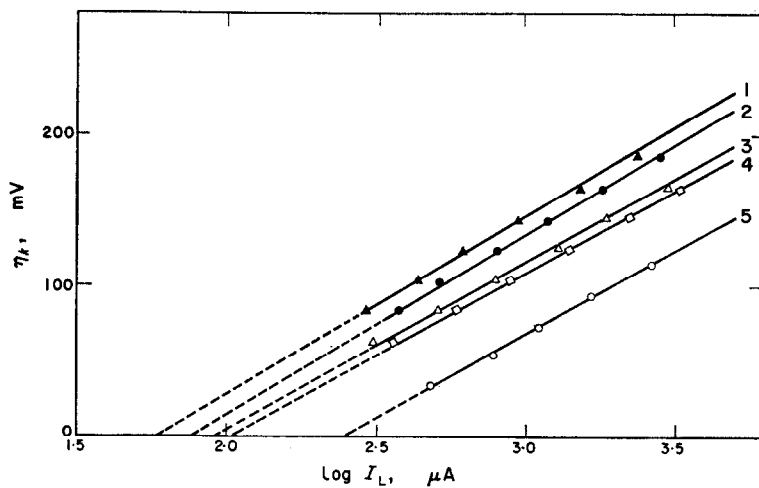
FIG. 19. Tafel plots. Oxidation of tri-iodide ion.
$C_{NaClO_4} = 0.4$ M. 25°C.

	C_{I_2}	C_{NaI}
1	0·0095 M	0·0080 M
2	0·0148 M	0·0127 M
3	0·0177 M	0·0124 M
4	0·0185 M	0·0110 M
5	—	0·0184 M
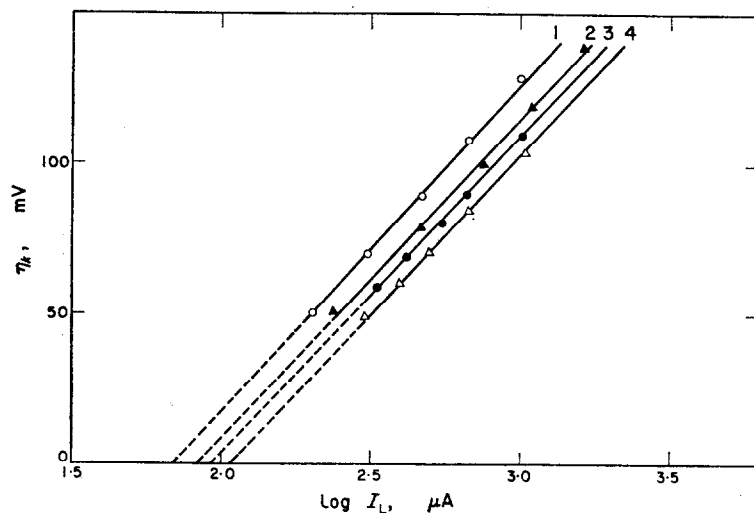
FIG. 20. Tafel plots. Reduction of iodine.
$C_{NaClO_4} = 0.4$ M. 25°C.

	C_{I_2}	C_{NaI}
1	0.0151 M	0.0081 M
2	0.0160 M	—
3	0.0177 M	0.0124 M
4	0.0200 M	0.0122 M
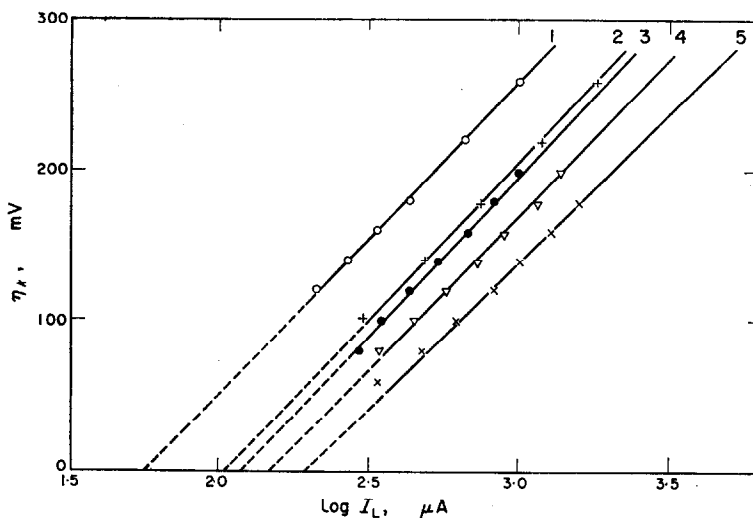
FIG. 21. Tafel plots. Reduction of tri-iodide ion.
$C_{NaClO_4} = 0.4$ M. 25°C.

	C_{I_2}	C_{NaI}
1	0.0024 M	0.0275 M
2	0.0113 M	0.0251 M
3	0.0148 M	0.0127 M
4	0.0185 M	0.0110 M
5	0.0194 M	—

TABLE 4. KINETIC PARAMETERS. ANODIC REACTIONS

IODIDE-ION OXIDATION

C_{I_2} M	C_{I^-} M	Temp. °C	p	$(b_T)_{1,a} \times 10^3$ V	$(\alpha)_{1,a}$	$(i_0)_{1,a} \times 10^3$ A/cm²
0·0023	0·0244	25·2	1·00	137	0·43	0·62
0·0024	0·0275	24·9	0·96	140	0·42	0·73
0·0151	0·0250	25·0	1·00	140	0·42	0·84
0·0113	0·0251	25·1	1·02	122	0·48	1·05
0·0187	0·0252	25·0	0·97	120	0·50	1·20
—	0·0095	30·3	0·97	120	0·50	0·49
—	0·0184	25·1	1·14	120	0·50	0·89
—	0·0080	25·2	0·80	120	0·50	0·69

TRI-IODIDE-ION OXIDATION

C_{I_2} M	C_{I^-} M	Temp. °C	p	$(b_T)_{2,a} \times 10^3$ V	$(\alpha)_{2,a}$	$(i_0)_{2,a} \times 10^3$ A/cm²
0·0095	0·0081	25·0	0·98	115	0·51	0·85
0·0148	0·0127	24·8	1·04	118	0·50	1·12
0·0151	0·0081	25·0	1·07	115	0·52	1·32
0·0177	0·0124	25·1	1·23	110	0·54	1·42
0·0185	0·0110	25·0	0·98	108	0·54	1·47
0·0208	0·0097	25·0	1·00	105	0·57	2·22
0·0201	0·0122	24·9	1·10	115	0·51	1·74
0·0187	0·0251	25·0	1·03	120	0·49	1·96
0·0023	0·0244	25·2	0·97	122	0·49	1·38
—	0·0184	25·1	1·01	112	0·53	3·72
—	0·0095	30·3	0·95	125	0·48	1·08
—	0·0080	25·2	1·00	120	0·48	4·70

TABLE 5. KINETIC PARAMETERS. CATHODIC REACTIONS

IODINE REDUCTION

C_{I_2} M	C_{I^-} M	Temp. °C	p	$(b_T)_{1,c} \times 10^3$ V	$(\alpha)_{1,c}$	$(i_0)_{1,c} \times 10^3$ A/cm²
0·0151	0·0081	25·1	0·97	115	0·51	1·05
0·0177	0·0124	24·9	0·95	110	0·54	1·26
0·0200	0·0122	25·0	0·94	108	0·55	1·52
0·0208	0·0097	25·0	1·03	110	0·54	1·95
0·0185	0·0110	25·1	0·96	110	0·54	1·63
0·0194	—	25·4	1·18	115	0·51	1·12
0·0133	—	25·1	1·02	123	0·48	1·35
0·0160	—	25·0	1·03	110	0·53	1·26
0·0093	—	28·5	1·13	118	0·50	1·47
0·0234	—	25·0	0·95	130	0·45	1·18

TRI-IODIDE-ION REDUCTION

C_{I_2} M	C_{I^-} M	Temp. °C	p	$(b_T)_{2,c} \times 10^3$ V	$(\alpha)_{2,c}$	$(i_0)_{2,c} \times 10^3$ A/cm²
0·0024	0·0275	25·1	0·96	210	0·28	0·82
0·0151	0·0250	25·0	1·00	206	0·29	0·83
0·0187	0·0252	25·0	1·00	215	0·28	0·96
0·0133	0·0252	24·9	1·10	215	0·28	1·50
0·0148	0·0127	25·2	0·92	215	0·28	1·74
0·0201	0·0123	25·0	1·03	202	0·29	1·66
0·0093	—	28·9	0·98	230	0·26	2·02
0·0073	0·0315	25·0	1·09	210	0·28	1·83
0·0160	—	25·1	1·07	205	0·29	1·91
0·0177	0·0124	25·0	0·98	198	0·30	1·98
0·0185	0·0110	25·2	0·95	200	0·30	1·98
0·0208	0·0097	25·0	1·07	197	0·30	2·05
0·0133	—	25·1	0·98	200	0·30	2·20
0·0194	—	25·4	1·14	190	0·31	2·52
0·0023	0·0244	25·5	0·97	220	0·27	0·42

TABLE 6. ACTIVATION ENERGIES DERIVED FROM THE DEPENDENCE
OF $(I_0)_x$ ON T

Iodide-ion oxidation	5200 ± 500	cal/mol
Tri-iodide-ion oxidation	4860 ± 500	cal/mol
Iodine reduction	4400 ± 500	cal/mol
Tri-iodide-ion reduction	4600 ± 500	cal/mol

temperature dependence of $(I_0)_x$ are presented in Table 6. The magnitudes of the four exchange cds are nearly the same.
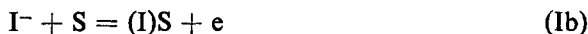
Possible reaction paths related to the anodic and cathodic processes

The possible reaction paths are presented considering first each process involved in the anodic and cathodic wave.

First anodic wave. Let us start with the first anodic wave where the reaction depends principally on the iodide ion concentration. Considering the reaction mechanisms already postulated for the discharge of halide ions in aqueous solutions[11-13] and the formal analogy with the mechanisms for the hydrogen evolution reaction,[14] the following reaction schemes for the iodide ion discharge are presented:

$$I^- + S = (I)S + e \tag{Ia}$$

$$(I)S + (I)S = I_2 + 2S \tag{IIa}$$

$$(I_2 + I^- = I_3^-) \tag{IIIa}$$

and

$$I^- + S = (I)S + e \tag{Ib}$$

$$(I)S + I^- = I_2 + S + e \tag{IIb}$$

$$(I_2 + I^- = I_3^-). \tag{IIIb}$$

where S represents an active site on the metallic electrode surface. From the kinetic standpoint reaction schemes *a* and *b* offer various possibilities as far as the rate determining step is concerned. To deal with these possibilities a quasi-steady state for the concentration of reaction intermediates is assumed.

Case (i). Reaction Ia is the rate determining step followed by reaction IIa. Let $\bar{C}_{I^-}$ and $\bar{C}_{I_2}$ respectively by the iodide-ion and iodine concentration in the electrical double layer; $C_{I(S)}$, the concentration of iodine atoms on the electrode surface; X, the degree of surface coverage by iodine atoms. The overvoltage η is actually equal to $\Delta\phi - \Delta\phi_R$, where $\Delta\phi$ is the difference between the potential, ϕ_M, and the outer potential, ϕ_s[15] and $\Delta\phi_R$, is the same difference at equilibrium. Assuming a symmetrical reaction co-ordinate ($\beta = 0.5$) the rate equations for each step are respectively

$$\vec{v}_{Ia} = \vec{k}_{Ia}\bar{C}_{I^-}(1 - X) \exp [\eta F/2RT] = \vec{A}_{Ia}(1 - X), \tag{12}$$

$$\overleftarrow{v}_{Ia} = \overleftarrow{k}_{Ia}X \exp [-\eta F/2RT] = \overleftarrow{A}_{Ia}X, \tag{13}$$

and

$$\vec{v}_{IIa} = \vec{k}_{IIa}X^2 = \vec{A}_{IIa}X^2. \tag{14}$$

Assuming furthermore that the rate of dissociation of molecular iodine at sufficiently

high overvoltages is negligible, if a quasi-steady state is established and reaction is the rate determining step, we have

$$\vec{A}_{\mathrm{IIa}} \gg \vec{A}_{\mathrm{Ia}} + \overleftarrow{A}_{\mathrm{Ia}} \tag{15}$$

and

$$\vec{A}_{\mathrm{Ia}} > \overleftarrow{A}_{\mathrm{Ia}}, \tag{16}$$

yielding

$$X = \left(\frac{\vec{A}_{\mathrm{Ia}}}{2\vec{A}_{\mathrm{IIa}}} \right)^{1/2}. \tag{17}$$

Therefore, the rate equation in terms of the cd is

$$\vec{I} = F\vec{k}_{\mathrm{Ia}}\bar{C}_{\mathrm{I^-}} \exp \left[\eta F/2RT \right]. \tag{18}$$

As the rotation speed approaches infinite, (18) becomes

$$\vec{I}_L = F\vec{k}_{\mathrm{Ia}}C_{\mathrm{I^-}} \exp \left[\eta F/2RT \right]. \tag{19}$$

Hence, the Tafel slope, b_{T}, for case (i), under a negligible surface coverage by reaction intermediates, is $2RT/F$ and a first-order reaction with respect to iodide-ion concentration is obtained. Equation (19) thus agrees in principle with the experimental findings.

Case (ii). Reaction IIa is the rate determining step preceded either by Ia or Ib. The kinetic analysis of case (ii) leads to second-order kinetics with respect to iodide ion and a Tafel slope equal to $RT/2F$. Consequently case (ii) must be discarded as a possible reaction mechanism.

Case (iii). Step Ib is rate determining, followed by IIb. The rate equations related to each step are

$$\vec{v}_{\mathrm{Ib}} = \vec{A}_{\mathrm{Ib}}(1 - X), \tag{20}$$

$$\overleftarrow{v}_{\mathrm{Ib}} = \overleftarrow{A}_{\mathrm{Ib}}X, \tag{21}$$

and

$$\vec{v}_{\mathrm{IIb}} = \vec{k}_{\mathrm{IIb}}\bar{C}_{\mathrm{I^-}}X \exp \left[\eta F/2RT \right] = \vec{A}_{\mathrm{IIb}}X. \tag{22}$$

Under a quasi-steady state for X, and taking into account (20) and (21), (22) becomes

$$X = \frac{\vec{A}_{\mathrm{IIb}}\vec{A}_{\mathrm{Ib}}}{\vec{A}_{\mathrm{Ib}} + \overleftarrow{A}_{\mathrm{Ib}} + \vec{A}_{\mathrm{IIb}}}. \tag{23}$$

If Ib is the rate-determining step and the intermediate desorption occurs through reaction IIb, the corresponding rate equation in terms of cd is

$$\vec{I}_L = 2F\vec{k}_{\mathrm{Ib}}C_{\mathrm{I^-}} \exp \left[\eta F/2RT \right]. \tag{24}$$

This equation is similar to that derived for case (i), again agreeing with the experimental results.

Case (iv). Reaction IIb is rate-determining, preceded either by Ia or Ib. This mechanism is represented by the following conditions

$$\vec{A}_{\mathrm{IIb}} \ll \vec{A}_{\mathrm{Ib}} + \overleftarrow{A}_{\mathrm{Ib}} \tag{25}$$

and

$$\overleftarrow{A}_{\mathrm{Ib}} < \vec{A}_{\mathrm{Ib}}, \tag{26}$$

where the latter implies a high degree of surface coverage. Taking into account (25) and (26) in (23), the rate equation is

$$\vec{I}_L = 2F\vec{k}_{\text{IIb}}C_{\text{I}^-}\exp[\eta F/2RT], \tag{27}$$

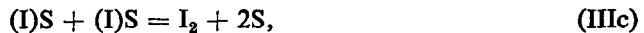involving again first-order kinetics with respect to iodine concentration and a Tafel slope of $2RT/F$.

On the other hand, if a low degree of surface coverage prevails, $\vec{A}_{\text{Ib}} < \overleftarrow{A}_{\text{Ib}}$, and the rate equation becomes

$$\vec{I}_L = 2F\frac{\vec{k}_{\text{Ib}}}{\overleftarrow{k}_{\text{Ib}}}\vec{k}_{\text{IIb}}C_{\text{I}^-}{}^2\exp[3\eta F/2RT]. \tag{28}$$

The latter comprises second-order kinetics with respect to iodide ion concentration and a Tafel slope of $2RT/3F$.

Second anodic wave. Formally the same mechanisms already analysed for the first anodic wave are also valid for the second, corresponding to the discharge of tri-iodide ion.

Considering total reaction (3) and equilibrium (1), the following set of consecutive reactions are very likely related to the oxidation of tri-iodide ion:

$$(2I_3^- = 2I_2 + 2I^-), \tag{Ic}$$

$$I^- + S = (I)S + e, \tag{IIc}$$

$$(I)S + (I)S = I_2 + 2S, \tag{IIIc}$$

and

$$(2I_3^- = 2I_2 + 2I^-), \tag{Id}$$

$$I^- + S = (I)S + e, \tag{IId}$$

$$I^- + (I)S = I_2 + S + e. \tag{IIId}$$

Both reaction schemes comprise the initial dissociation of the complex ion, which stability is determined by the equilibrium constant, K_{I}, defined as

$$K_{\text{I}} = \frac{\bar{C}_{\text{I}_2} \times \bar{C}_{\text{I}^-}}{\bar{C}_{\text{I}_3^-}}. \tag{29}$$

The rate equations previously derived can be extended to the reaction involved in the second anodic wave as follows.

Case (i). If either reaction IIc or IId is rate-determining, followed by IIIc or IIId respectively, the corresponding rate equations are

$$\vec{I}_L = FK_{\text{I}}\vec{k}_{\text{IIc}}\frac{C_{\text{I}_3^-}}{C_{\text{I}_2}}\exp[\eta F/2RT], \tag{30}$$

or

$$\vec{I}_L = 2F\vec{k}_{\text{IIc}}C_{\text{I}^-}\exp[\eta F/2RT]. \tag{31}$$

Case (ii). Reaction IIId is rate-determining. For a degree of coverage approaching 1, the rate equation is

$$\vec{I}_L = 2FK_{\text{I}}\vec{k}_{\text{IIId}}\frac{C_{\text{I}_3^-}}{C_{\text{I}_2}}\exp[\eta F/2RT] \tag{32}$$

and, on the other hand, for a degree of coverage approaching zero, it is

$$\overrightarrow{I_L} = 2FK_I\overleftarrow{k}_{IIIa} \frac{C_{I_3^-}^2}{C_{I_2}^2} \exp [3\eta F/2RT]. \tag{33}$$

Equations (31) and (32) yield, in principle, kinetic parameters which agree with those experimentally derived.

First cathodic wave. The likely reaction schemes involved in the electrochemical reduction of molecular iodine are those comprising the reverse reactions already described for the oxidation of tri-iodide ion, according to the total reaction (4).

Case (i). Reaction IIc is the rate determining step preceded by step IIIc. If the degree of surface coverage approaches 1, then the rate equation is

$$\overleftarrow{I_L} = 2F\overleftarrow{k}_{IIc} \exp [-\eta F/2RT], \tag{34}$$

which predicts a zero-order reaction with respect to iodine concentration On the contrary, if the degree of surface coverage approaches 0, the rate equation is

$$\overleftarrow{I_L} = 2F \left(\frac{\overleftarrow{k}_{IIIc}}{4\overrightarrow{k}_{IIIc}}\right) \overleftarrow{k}_{IIc} C_{I_2}^{1/2} \exp [-\eta F/2RT], \tag{35}$$

which indicates a half-order reaction with respect to iodine concentration. Neither (34) nor (35) agree with the experimental results.

Case (ii). Reaction IId is rate-determining, preceded by reaction IIId. Applying the previous procedure, the following limiting rate equations are obtained, respectively, when $X \to 1$ and $X \to 0$,

$$\overleftarrow{I_L} = 2F\overleftarrow{k}_{IId} \exp [-\eta F/2RT] \tag{36}$$

and

$$\overleftarrow{I_L} = 2F \frac{\overleftarrow{k}_{IIId}}{\overrightarrow{k}_{IIId}} \overleftarrow{k}_{IId} \frac{C_{I_2}}{C_{I^-}} \exp [-3\eta F/2RT]. \tag{37}$$

Case (iii). Reaction IIId is rate-determining, followed by IId. The rate equation is

$$\overleftarrow{I_L} = 2F\overleftarrow{k}_{IIId} C_{I_2} \exp [-\eta F/2RT], \tag{38}$$

involving a Tafel slope equal to $2RT/F$ and first-order kinetics with respect to iodine concentration.

Second cathodic wave. As regards the second cathodic wave, the same considerations as for the second anodic wave apply. If reaction IIIb is in equilibrium and scheme b comprising reaction IIb as rate-determining step is obeyed, the rate equation for the process involved is

$$\overleftarrow{I_L} = 2FK_I\overleftarrow{k}_{IIb} \frac{C_{I_3^-}}{C_{I^-}} \exp [-\eta F/2RT]. \tag{39}$$

It implies first-order kinetics with respect to tri-iodide ion concentration, as experimentally observed, and a Tafel slope of $2RT/F$.

Mechanisms of the iodide–tri-iodide–iodine electrode in ACN

To explain the kinetics of the iodide–tri-iodide–iodine electrode in ACN, in terms of a reaction mechanism, the anodic and cathodic processes must be considered as

complementary processes. This implies that the anodic and cathodic reaction mechanisms must involve the same reaction either in the one or in the other direction as the rate-determining step. Furthermore, if the occurrence of two anodic and cathodic waves is due principally to equilibrium reaction (1), which is fast enough as compared to other reactions, the same rate-determining step should be responsible for the kinetic behaviour of all the reactions comprised in the four waves observed in the current/voltage curves. After these considerations, deduced from the experimental facts, it appears that the processes involved in the first anodic and in the second cathodic waves are satisfactorily interpreted by the reaction scheme b, comprising, under a high degree of coverage at large anodic overvoltages, reaction IIb as the rate-determining step. Similarly the processes related with the second anodic wave and the first cathodic wave occur very likely according to the reaction scheme d, involving reaction IIId as the rate-determining step. Hence, only one rate-determining step, for the forward and reverse direction, produces the kinetic control of the electrode processes as a whole. These mechanisms satisfy also first-order kinetics with respect to the reacting species as found in the experiments, and the acceptable coincidence of the exchange cds.

Reaction mechanisms b (IIb) and d (IIId) imply a stoichiometric number, ν^*, equal to 1. This number is actually obtained with the Tafel slope and the relationship

$$\nu^* = \frac{b_{\mathrm{T}}F(n_a + n^{\ddagger}\beta)}{RT}, \tag{40}$$

where $n^{\ddagger}$ is the number of electrons transferred in the steps preceding the rate-determining step and n_a the number of electrons participating in the latter. In applying equation (40), Tafel slopes equal to $2RT/F$ are taken for both cathodic reactions, while for the anodic reactions the slope $2RT/3F$ must be considered for referring the complementary reactions to the same degree of surface coverage.

No full coincidence between the theoretical kinetic parameters and the experimental ones is however observed, as the Tafel slope related to tri-iodide ion reduction is nearly twice the predicted value. This anomalous slope on the other hand must be related to the hysteresis effect observed in the current/voltage curve.

A possible interpretation of the high cathodic Tafel slope in terms of an unsymmetrical reaction co-ordinate is unacceptable, since the effect is absent in the complementary anodic reaction, as deduced from its Tafel slope. Consequently the difference of the theoretical and experimental second cathodic Tafel slopes should be assigned to an additional process interfering with the electron-transfer reaction at high cathodic overvoltages.

A Tafel slope of about $4RT/F$ could be due to a film formation on the electrode surface,[16] which causes an additional energy barrier to the electron-transfer reaction. Film formation, within the cathodic overvoltage region, in the present circumstances might be related in part to the fact that at negative potentials the ionic reacting species are repelled from the electrical double layer, yielding an accumulation of neutral species, either iodine atoms or molecules, on the electrode surface. A reverse type of interaction between the electrode surface and the ionic species must occur during the anodic reactions; no hysteresis is then observed. Hysteresis is thus a typical effect of the cathodic reaction.

However, if the accumulation of either iodine atoms or molecules is the principal cause of the hysteresis, it is difficult to imagine in the rotating disk electrode how the hysteresis loop increases with the sweep rate of potential. Furthermore this hypothesis suggests that the same sort of effect should occur with the same reaction in other aprotic solvents, but this is not the case, as far as DMSO is concerned, where the hysteresis observed in the second cathodic wave is just the reverse.[17] These facts favour an interpretation based on a non-conducting film formation. Therefore the hysteresis must, in the present case, be closely related to a passive state on the electrode at the higher cathodic overvoltages reached in the experiments. Undoubtedly, this permanent passivation is caused by a poorly conducting film, as the activity of the electrode is recovered by just repolishing its surface. The existence of the effect is not surprising, since at very high cathodic overvoltages electrochemical decomposition of the solvent takes place. Particularly for ACN, radicals formed by molecule decomposition react, yielding under certain conditions organic polymers. If this type of reaction also occurs on the electrode, it would explain the fact that oxygen prevents the film formation. Oxygen may react in two distinct ways, probably simultaneously. Either it is reduced on the platinum cathode or it acts as a scavenger of radicals yielded by solvent decomposition, avoiding thus the formation of a non-conducting film on the electrode.

It is probable that the above mentioned complication, related principally to tri-iodide reduction, involves also a further contribution of non-homogeneity of the electrode surface, as suggested for aqueous solutions,[11] related perhaps to its state of oxidation. Nevertheless under the present experimental conditions no reliable conclusion can be drawn as far as this point is concerned.

Finally, the conclusion is that the reaction mechanism related to the four waves found in the current/voltage curves are formally analogous, probably involving a symmetrical reaction co-ordinate and the participation of the same activated complex. It is also very likely that the same reaction mechanisms apply to the kinetics of the iodine–tri-iodide–iodide electrode in other organic solvents, particularly dimethyl-sulphoxide.[17]

REFERENCES

1. R. T. IWAMOTO, *Analyt. Chem.* **31**, 955 (1959).
2. M. C. GIORDANO, J. C. BAZÁN and A. J. ARVÍA, *Electrochim. Acta* **11**, 1553 (1966).
3. M. C. GIORDANO, J. C. BAZÁN and A. J. ARVÍA, *Electrochim. Acta* **12**, 723 (1967).
4. A. I. POPOV and D. H. GESKE, *J. Am. chem. Soc.* **80**, 1340 (1958).
5. I. V. NELSON and R. T. IWAMOTO, *J. electroanal. Chem.* **7**, 218 (1964).
6. J. DESBARRES, *Bull. Soc. Chim. France* 502 (1961); A. J. PARKER, *J. chem. Soc. (London)* A 220 (1966).
7. R. GUIDELLI and G. P. PICCARDI, *Electrochim. Acta* **12**, 1085 (1967).
8. A. J. ARVÍA, S. L. MARCHIANO and J. J. PODESTÁ, *Electrochim. Acta* **12**, 259 (1967).
9. V. G. LEVICH, *Physiochemical Hydrodynamics.* Prentice-Hall, Englewood Cliffs, N.J. (1962).
10. A. FRUMKIN and G. TEDORADSE, *Z. Elektrochem.* **62**, 251 (1958).
11. J. D. NEWSON and A. C. RIDDIFORD, *J. electrochem. Soc.* **108**, 695 (1961); **108**, 699 (1961).
12. K. J. VETTER, *Z. phys. Chem.* **199**, 22, **199**, 185 (1952).
13. J. JORDAN and R. A. JAVICK, *J. Am. chem. Soc.* **80**, 1264 (1958).
14. J. O'M. BOCKRIS, *Modern Aspects of Electrochemistry.* Butterworths, London (1954).
15. B. E. CONWAY, *Theory and Principles of Electrode Processes.* Ronald Press, New York (1965).
16. A. DAMJANOVIC, A. DEY and J. O'M. BOCKRIS, *Electrochim. Acta* **11**, 791 (1966).
17. A. J. ARVÍA, M. C. GIORDANO and J. J. PODESTÁ, *Electrochim. Acta* in press.